*Thermochimica Acta*, 153 (1989) 193–204
Elsevier Science Publishers B.V., Amsterdam – Printed in The Netherlands


# PREPARATION AND THERMAL STABILITY OF MANGANESE OXIDES OBTAINED BY PRECIPITATION FROM AQUEOUS MANGANESE SULPHATE SOLUTION

J. PATTANAYAK * and V. SITAKARA RAO

*Department of Chemistry, Indian Institute of Technology, Kharagpur 721302 (India)*

H.S. MAITI

*Electro-Ceramics Division, Central Glass and Ceramics Research Institute, Jadavpur, Calcutta 700032 (India)*

(Received 22 February 1989)

## ABSTRACT

Precipitated products of hydrolysis of manganese sulphate with sodium hydroxide were obtained by adding manganese sulphate solution to boiling solutions of sodium hydroxide of varying pH. The products are $Mn_3O_4$ at pH 9, $\gamma$-$Mn_2O_3$ at pH 13, and possibly a mixture of $Mn_3O_4$ and $\gamma$-$Mn_2O_3$ at pH 10. DTA of $Mn_3O_4$ prepared at pH 9 shows two endothermic peaks, at 70 and 965 °C, and two exothermic peaks, at around 180 and 655 °C. TG analysis of the sample indicates continuous weight loss from 30 to 600 °C, considerable weight gain beyond this, and then a further abrupt loss in weight above 960 °C. On heating, $Mn_3O_4$ oxidizes to $\alpha$-$Mn_2O_3$ above 600 °C, possibly through an intermediate phase of $\gamma$-$Mn_2O_3$, which on further heating reduces to $Mn_3O_4$ above 960 °C. Specimens prepared at pH 10 consist of a mixture of $Mn_3O_4$ and $\gamma$-$Mn_2O_3$, whose thermal transformations are nearly identical to those of $Mn_3O_4$. However, $\gamma$-$Mn_2O_3$ prepared at pH 13 goes through a quite different thermal transformation sequence. DTA of this sample shows a broad endotherm at around 70 °C and an equally broad exotherm at around 320 °C. The corresponding TG curve shows weight loss from 30 to 750 °C through a number of distinct steps. On heating, $\gamma$-$Mn_2O_3$ loses moisture up to 450 °C, and above this temperature it converts to $Mn_3O_4$.

## INTRODUCTION

The transition metal manganese exists in a number of different oxidation states. Because of its many easily convertible valency states, it forms one of the most complex oxide systems [1]. The ready valency change of manganese leads to the formation of a large number of oxides of varying degrees of stability. The thermal behaviour of these oxides strongly depends on the particular experimental conditions [2].

* Present address: Central Research Facility, I.I.T., Kharagpur-721302, West Bengal, India.

0040-6031/89/$03.50 

The possible valency states of manganese give rise to lower oxides, such as manganese sesquioxide ($Mn_2O_3$) and hausmannite ($Mn_3O_4$). The former exists in two forms, designated as $\alpha$ and $\gamma$ forms. The $\gamma$ form, however, is very unstable [3,4]. Both $\gamma$-$Mn_2O_3$ and $Mn_3O_4$ have an identical crystal structure, as in the case of $\gamma$-$Fe_2O_3$ and $Fe_3O_4$ [5]. These oxides have a pseudo-spinel structure with tetragonal symmetry. They have identical axial ratios of 1 : 16, and the cations at tetrahedral sites are surrounded by four equidistant oxygen ions [6]. Both these oxides can be represented by the formula $Mn^{2+}[Mn_2^{3+}]O_4$, where the ions between the square brackets are at the octahedral sites of the spinel [7]. Because of the close similarities between the structures of these two oxides, the X-ray diffraction (XRD) pattern of $\gamma$-$Mn_2O_3$ is nearly identical to that of $Mn_3O_4$ [3,4].

$Mn_3O_4$ is generally prepared by reduction of higher manganese oxides or by thermal decomposition of divalent manganous salts (e.g. the nitrate, carbonate or oxalate) in air at around 1000 °C [3,8]. It has been reported [9] that addition of an alkali to an aqueous $Mn^{2+}$ salt solution produces $Mn(OH)_2$, the outer layer of which in the presence of atmospheric oxygen is immediately converted to $Mn_3O_4$. On further exposure of the $Mn(OH)_2$ to air, a second layer of $Mn_2O_3$ is also formed. In this way, Beller and Seddon [10] and Jerez and Alario [11] have prepared readily filterable $Mn_3O_4$ by brief oxidation of manganese hydroxide in air. $\gamma$-$Mn_2O_3$, however, is very unstable and so cannot be prepared easily from aqueous $Mn^{2+}$ solution or by oxidation/reduction of manganese oxides of lower/higher state. Very few experimental methods have been reported for the preparation of $\gamma$-$Mn_2O_3$. Moore et al. [3] have suggested two methods of preparation. The first method involves the oxidation of a dilute solution of manganous sulphate with hydrogen peroxide. In the second method, $\gamma$-$Mn_2O_3$ is formed by heating $\gamma$-$MnO_2$ at 500 °C under vacuum for about 78 h. Braner [12] and Hernann et al. [13] have used the second method, preparing the $\gamma$-$Mn_2O_3$ by dehydration of $\gamma$-MnOOH in a vacuum.

It has been reported that $\gamma$-$Mn_2O_3$ can be converted to $\alpha$-$Mn_2O_3$ on heating in vacuum at 500 °C, or on standing for a year at room temperature [3,4]. When heated at 250 °C in an oxygen atmosphere for 100 h, the structure of $\gamma$-$Mn_2O_3$ becomes highly disordered without forming any new phase [3]. But when $Mn_3O_4$ is heated in air within the thermal stability range of $Mn_2O_3$ (500–1000 °C), slow oxidation to $\alpha$-$Mn_2O_3$ occurs [14]. Dollimore and Tonge [15] have studied the thermal behaviour of synthetic manganese oxides, and reported that the sequence of transformation of $Mn_3O_4$ to $\alpha$-$Mn_2O_3$ takes place via an intermediate phase of $\gamma$-$Mn_2O_3$.

In the present work, both $\gamma$-$Mn_2O_3$ and $Mn_3O_4$ were prepared from aqueous $Mn^{2+}$ solution by precipitation. Attempts have been made to characterize the thermal transformations by various experimental techniques.

## EXPERIMENTAL

Manganese oxides were prepared by slowly adding 0.1 M manganese sulphate (G.R.) solution to a freshly prepared and continuously stirred boiling solution of sodium hydroxide (A.R.) under pH conditions of 9, 10 and 13. However, because of the ready valency change of manganese ions in alkaline medium, manganese(II) hydroxide was converted to different forms of manganese oxide on contact with air. The precipitation was over within 1 h. Conditions of pH 9 and 10 were precisely controlled using a digital pH meter with a special glass electrode. However, control of pH above this value was quite difficult, particularly in boiling conditions, and the problem was exacerbated by the uncertainty of pH measurement using a glass electrode. To ensure a pH of more than 10, a significantly higher concentration (2.5 N) of alkali was used, which helped to raise the pH of the solution to around 13. However, the actual pH may not have been exactly 13. The reproducibility of the precipitate was checked by repeating the process several times. The precipitate was then washed repeatedly with distilled water until the washings were free from adsorbed impurity ions. The residue was then dried in air. The absence from the precipitates of appreciable amounts of sodium was confirmed using a digital flame photometer. The pure manganese oxide samples prepared at pH 9, 10 and 13 were designated SA, SB and SC, respectively.

The elemental compositions of manganese present in the specimens prepared under the various pH conditions, were determined by the bismuthate method. The principle of the process depends upon the fact that under certain conditions bivalent manganese ions can be quantitatively oxidized to permanganic acid by sodium bismuthate

$$2Mn^{2+} + 5NaBiO_3 + 14H^+ \rightarrow 2MnO_4^- + 5Na^{2+} + 7H_2O + 5Bi^{3+}$$

The permanganic acid was then titrated using standard ferrous sulphate solution, and the amount of manganese calculated using the relation 1000 ml N $KMnO_4 \equiv 10.99$ g Mn.

Thermal analysis of the air-dried sample was carried out in a Stanton–Redcroft STA-780 and a DuPont 910 thermal analyser using a suitable quantity of the sample (20–25 mg).

A Perkin–Elmer 983 IR spectrophotometer was used to record IR spectra of the samples in the range 200–4000 $cm^{-1}$, with either potassium bromide or polythene pellets.

XRD patterns of these samples were obtained using an X-ray diffractometer type JDX-8P (Jeol) operated at 30 kV and 15 mA. Fe $K\alpha$ radiation was used as the X-ray source.

Electron micrographs of the samples were taken using a Jem-200 CX (Jeol) electron microscope with a power rating of 100 kV and a camera length of 42 cm. The magnification of the microscope was adjusted to 48 000.

## RESULTS AND DISCUSSION

The powder XRD patterns of the SA, SB and SC samples are identical at room temperature. All the samples produce diffraction peaks which may be due to either $Mn_3O_4$ or $\gamma$-$Mn_2O_3$, which have identical patterns. Therefore, it was not possible to identify the exact nature of the compound solely from XRD patterns of the powders dried at room temperature. Although all the precipitates have the same XRD pattern, their thermal transformation behaviours were found to be significantly different. TG results, presented in Fig. 1, indicate that the thermal transformation behaviour of sample SA is distinctly different from that of SC. Sample SB is somewhat intermediate between the previous two, but its behaviour is comparatively closer to that of SA. On the assumption that samples SA and SB have nearly identical properties, sample SB was not studied in some of the later experiments. DTA results for samples SA and SC are given in Fig. 2, and the transmission electron micrographs for the same two samples are shown in Fig. 3. It is evident that there is a significant difference between the particle morphologies of the two specimens. The particles of sample SA (Fig. 3 (a)) are comparatively regular in shape but of finer grade, whereas sample SC (Fig. 3 (b)) consists of elongated needle-shaped crystallites. All these observations

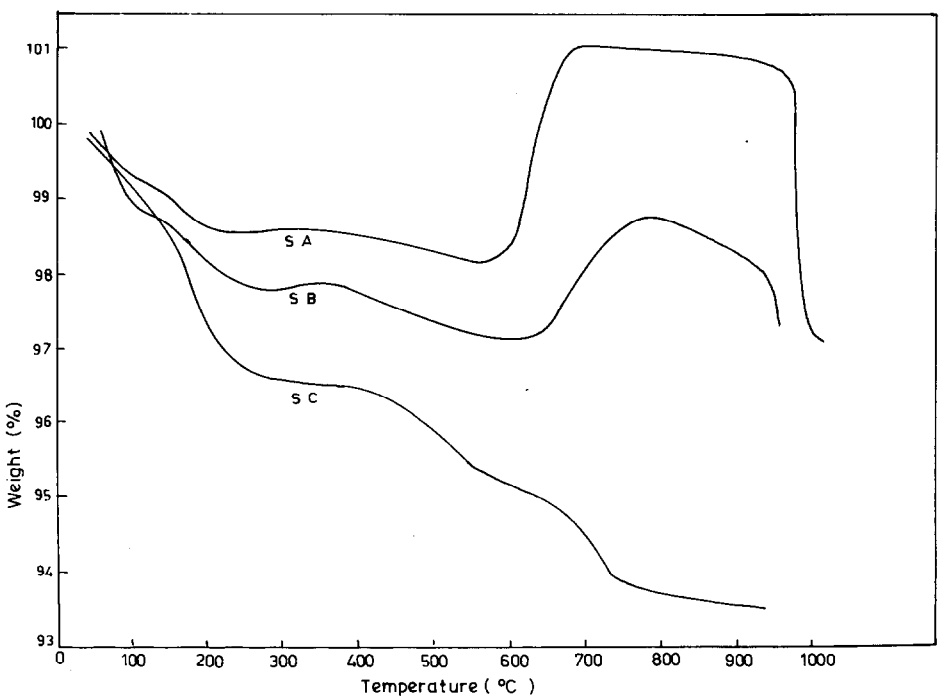


Fig. 1. TG curves for manganese oxide precipitated at pH 9 (SA), 10 (SB) and 13 (SC).

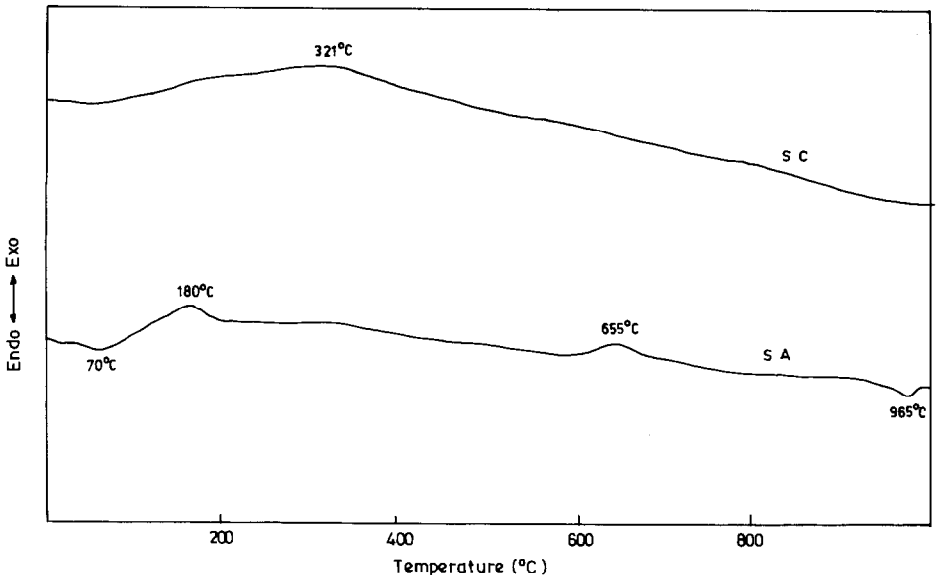


Fig. 2. DTA of manganese oxide precipitated at pH 9 (SA) and 13 (SC).

indicate that the samples prepared under the two different pH conditions do not have identical primary particles, even though they have identical XRD patterns.

Attempts were made to differentiate between the samples on the basis of their IR spectra, which are presented in Fig. 4. The spectra of samples SA and SB indicate the presence of two distinct absorption peaks, at 3400 and 1600 $cm^{-1}$, whereas the spectrum for sample SC indicates three distinct absorption peaks, at 3400, 1600 and 900 $cm^{-1}$. The peaks at 3400 and 1600 $cm^{-1}$ confirm the presence of water molecules in all the specimens. The band at 900 $cm^{-1}$ indicates the presence of lattice $OH^-$ ions in sample SC [16]. In the lower wavenumber range, the spectra of SA and SB show four

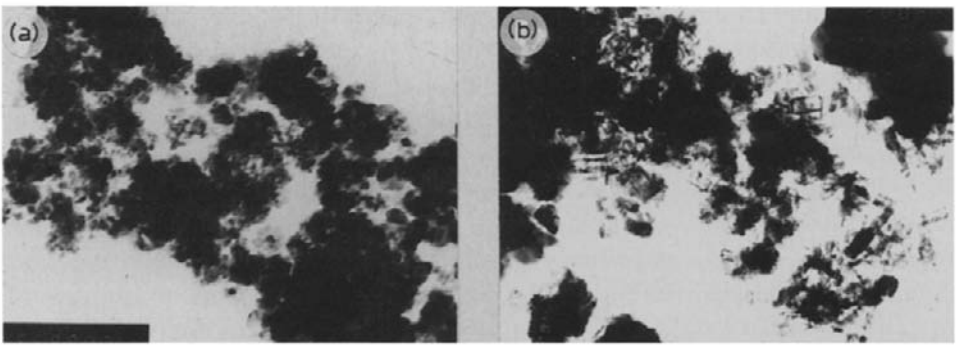


Fig. 3. Electron micrographs of manganese oxide precipitated (a) at pH 9 (SA), and (b) at pH 13 (SC).

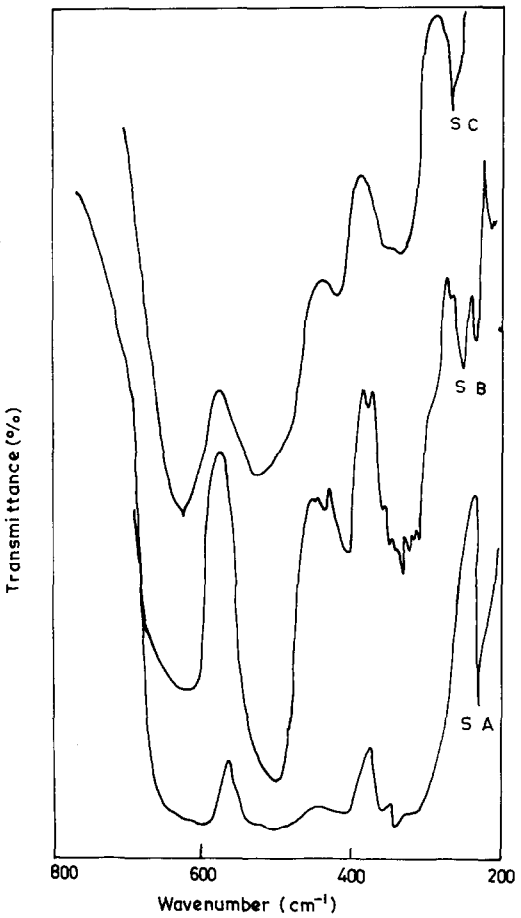


Fig. 4. IR spectra of manganese oxide precipitated at pH 9 (SA), 10 (SB) and 13 (SC).

transmittance peaks, at 580, 455, 390 and 260 $cm^{-1}$. The height of the peak at 580 $cm^{-1}$ is greater than that of the peak at 455 $cm^{-1}$. A comparison of the IR spectra of $Mn_3O_4$ and $\gamma$-$Mn_2O_3$ as given by Gattow and Glemser [17] reveals that in the case of $Mn_3O_4$, the transmittance peak at 580 $cm^{-1}$ is comparatively higher than the same peak at 455 $cm^{-1}$, while in the case of $\gamma$-$Mn_2O_3$, the peak at 455 $cm^{-1}$ is higher than the peak at 580 $cm^{-1}$. Hence, the particles of samples SA and SB must correspond to the $Mn_3O_4$ phase at room temperature. Sample SC also shows four transmittance peaks, at 570, 430, 375 and 270 $cm^{-1}$, at room temperature. But in this case the peak intensity at 430 $cm^{-1}$ is higher than that at 570 $cm^{-1}$, indicating the presence of $\gamma$-$Mn_2O_3$ as primary particles. The formation of two types of manganese oxide at different pH is also supported by chemical analyses of the samples, which indicate elemental manganese content for samples SA and SC of 73 and 67.6% respectively. These values are nearly equal to the theoretical estimates of manganese in $Mn_3O_4$ and $\gamma$-$Mn_2O_3$, respectively.

From the position and intensity of the IR peaks presented above, it can be concluded that samples SA and SC consist primarily of $Mn_3O_4$ and $\gamma$-$Mn_2O_3$ phase respectively, whereas sample SC possibly contains a mixture of these two phases.

The TG analysis of sample SA (Fig. 1) indicates continuous weight loss from 30 to 600 °C over three distinct steps. Above 600 °C there is a considerable gain in weight, up to 700 °C. A slight weight loss takes place between 700 and 960 °C, above which there occurs a further abrupt loss in weight. DTA of sample SA (Fig. 2) shows a broad endothermic peak at 70 °C and another small one at 965 °C. In addition, there are two exothermic peaks, at around 180 and 655 °C. The endothermic peak at 70 °C is due to the removal of loosely bound water. The IR spectra and XRD patterns of the samples heated at different temperatures up to 600 °C do not indicate any phase change (Figs. 5 and 6), but the IR spectra indicate

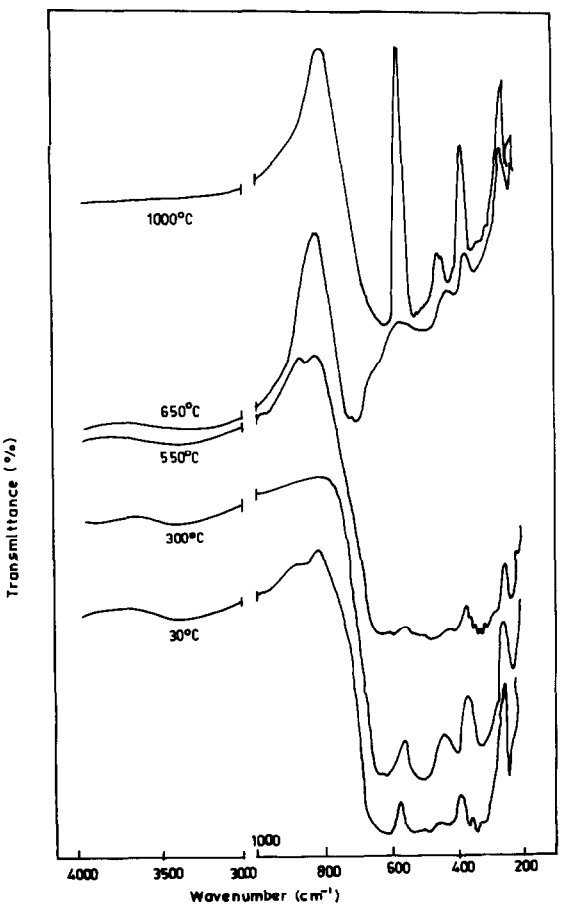


Fig. 5. IR spectra of manganese oxide precipitated at pH 9 (SA) and heated at different temperatures.

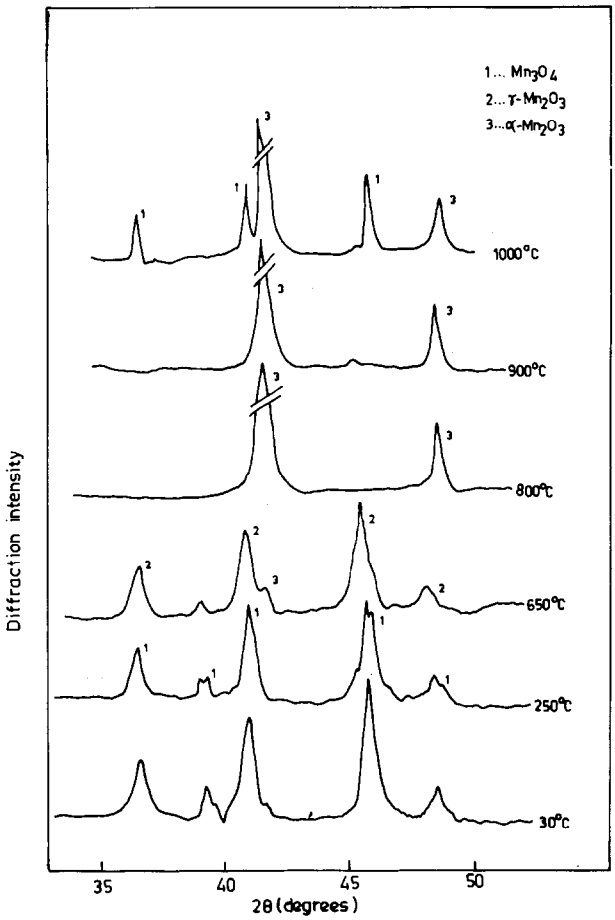


Fig. 6. XRD patterns of manganese oxide precipitated at pH 9 (SA) and heated at different temperatures.

removal of moisture during the heating process. So the weight loss up to 600 °C observed in the TG plot is primarily due to loss of different types of water, as proposed by Lee et al. [18] for the case of γ-$MnO_2$. The DTA peak at 180 °C is probably due to the release of stored energy resulting from the increase of crystallite size. XRD analysis of the sample heated at 600 °C indicates the formation of a small amount of α-$Mn_2O_3$ along with either $Mn_3O_4$ or γ-$Mn_2O_3$, while at 800 °C and 900 °C the patterns confirm the presence of α-$Mn_2O_3$ only (Fig. 6). From the IR spectra of the sample heated at 650 °C (Fig. 5) it can be seen that the transmittance peak at 430 $cm^{-1}$ is higher than that at 570 $cm^{-1}$. This confirms the presence of the γ-$Mn_2O_3$ phase (as discussed previously) at this temperature. From these observations it is clear that sample SA, which consists of $Mn_3O_4$ at room temperature, is oxidized to α-$Mn_2O_3$ above 600 °C, possibly through an intermediate phase of γ-$Mn_2O_3$ [9]. So the increase in weight in the TG

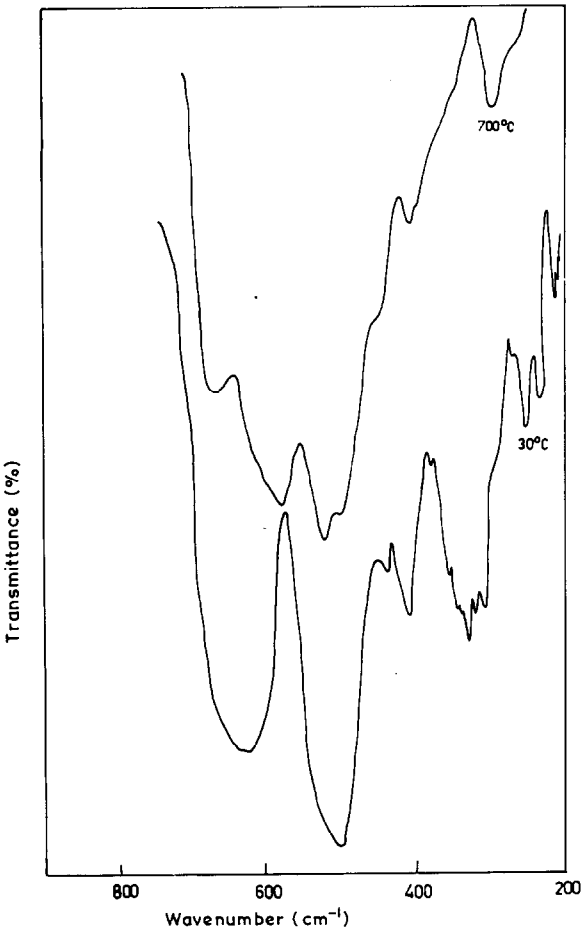


Fig. 7. IR spectra of manganese oxide precipitated at pH 10 (SB) and heated at different temperatures.

curve above 600 °C and the DTA peak at 655 °C are attributable to the conversion of $Mn_3O_4$ to $\alpha$-$Mn_2O_3$. IR and X-ray analyses of samples heated above 960 °C indicate the reappearance of $Mn_3O_4$, associated with sudden weight loss in the TG curve and an endothermic peak at 965 °C in the DTA plot.

From the TG analysis (Fig. 1), IR spectra (Fig. 7) and XRD pattern (same as Fig. 6) of sample SB at various temperatures, it is clear that, as expected, the sample undergoes thermal transformations which are nearly identical to those of sample SA. On the other hand, sample SC, which primarily contains $\gamma$-$Mn_2O_3$, goes through a quite different thermal transformation sequence.

The DTA plot of sample SC (Fig. 2) does not show very well defined peaks but it does show a broad endotherm at around 70 °C and an equally broad exotherm at around 320 °C. The TG curve (Fig. 1) shows weight loss

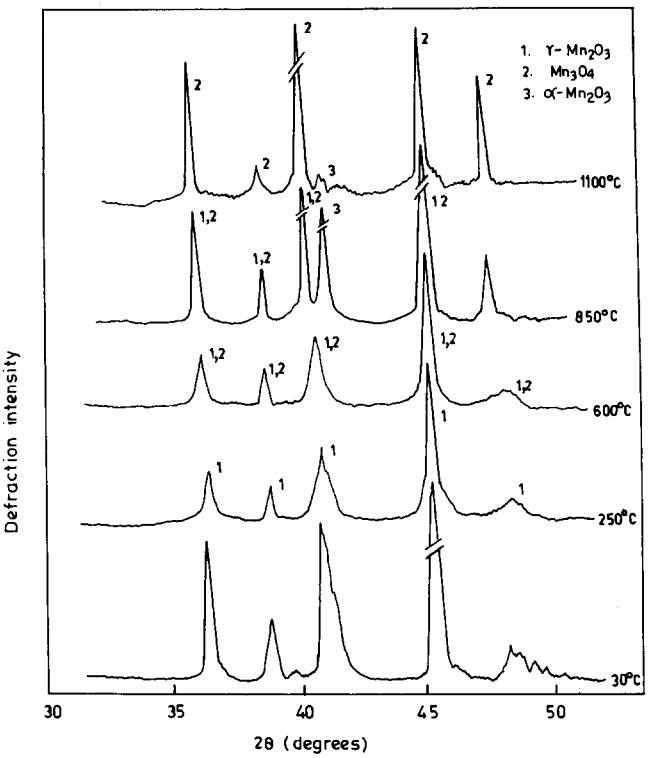


Fig. 8. XRD patterns of manganese oxide precipitated at pH 13 (SC) and heated at different temperatures.

from 30 to 750 °C in a number of distinct steps. The XRD patterns do not change, at least up to 800 °C (Fig. 8), indicating that either the primary particles of $\gamma$-$Mn_2O_3$ do not undergo any transformation during heating, or they slowly change to the $Mn_3O_4$ phase, which has XRD patterns identical to those of $\gamma$-$Mn_2O_3$. However, the IR spectra of the samples heated to different temperatures (Fig. 9) indicate that on heating from 30 to 800 °C there is a gradual change in the relative intensities of the two characteristic transmittance peaks at 550 and 450 $cm^{-1}$, suggesting that the primary particles of $\gamma$-$Mn_2O_3$ very slowly transform to $Mn_3O_4$, and the sample contains a mixture of $\gamma$-$Mn_2O_3$ and $Mn_3O_4$ at 800 °C, but finally converts to pure $Mn_3O_4$ above 1100 °C. The presence of $\alpha$-$Mn_2O_3$ in addition to $\gamma$-$Mn_2O_3$/$Mn_3O_4$ in the temperature range 850–1100 °C is confirmed by the XRD pattern. The gradual decrease of the intensities of the IR peaks at 3400, 1600 and 900 $cm^{-1}$ with increasing temperature of the sample up to 400 °C (Fig. 9) suggests slow elimination of moisture and hydroxyl ions during heating. Therefore, the loss in weight between 30 and 450 °C, as observed in the TG curve, is primarily due to removal of moisture, either adsorbed or present in the crystalline lattice. Further loss in weight on

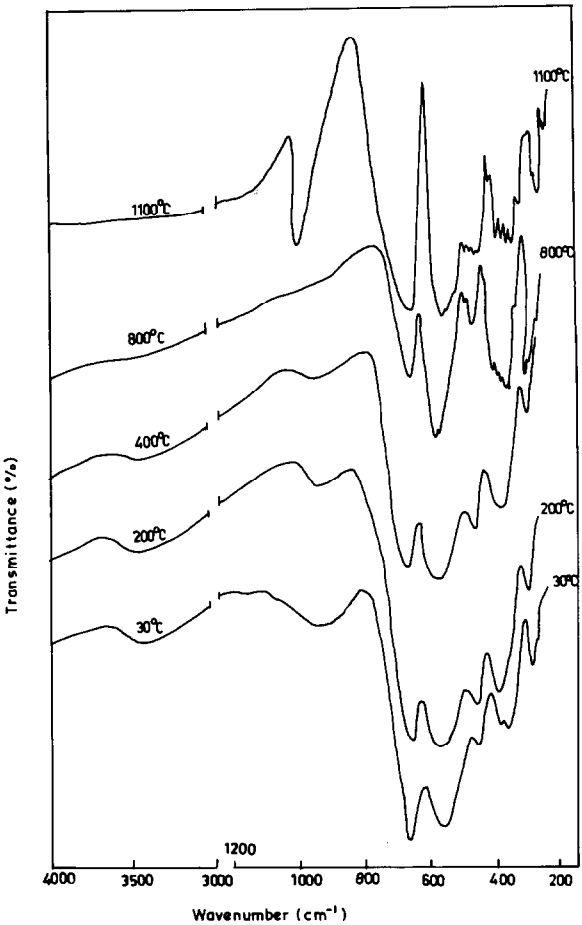


Fig. 9. IR spectra of manganese oxide precipitated at pH 13 (SC) and heated at different temperatures.

heating above 450 °C is probably due to removal of lattice oxygen, which is primarily responsible for the conversion of $\gamma$-$Mn_2O_3$ to $Mn_3O_4$.

## REFERENCES

1 O. Bricker, Am. Miner., 50 (1965) 1296.
2 R.C. McKenzie and G. Berggren, in R.C. McKenzie (Ed.) Differential Thermal Analysis, Academic Press, New York, 1970, p. 2.
3 T.E. Moore, M. Ellis and P.W. Selwood, J. Am. Chem. Soc., 72 (1950) 856.
4 W.C. Vosburgh, J. Electrochem. Soc., 106 (1959) 839.
5 A.F. Wells, Structural Inorganic Chemistry, Oxford University Press, London, 3rd edn., 1962.
6 K.P. Sinha and A.P.B. Sinha, J. Phys. Soc., 61 (1957) 758.
7 J.B. Goodenough and A.L. Loeb, Phys. Rev., 98 (1955) 391.

8 R.D.W. Kemmitt and R.D. Peacock, The Chemistry of Manganese, Technetium and Rhenium, Pergamon, Oxford, 1973.
9 B.A. Dzhanastivilli, E.N. Bogoyavlenskii and Kh.G. Purlseladze, Akad. Nauk Gruz. S.S.S.R., 43 (1966) 361.
10 M. Beller and W.L. Seddon, U.S. Patent 3,767,786 (1973).
11 A. Jerez and M.A. Alario, Thermochim. Acta, 58 (1982) 339.
12 G. Braner, Handbook of Preparative Inorganic Chemistry, Vol. 1, Academic Press, New York, 2nd edn., 1963, p. 2.
13 L. Hernann, J. Morales and J.L. Tirado, Surf. Coat. Technol., 27 (1986) 343.
14 G. Gyula, Acta Miner. Petrogr., 20 (1972) 227.
15 D. Dollimore and K.H. Tonge, Proc. Third ICTA, Davol, 2 (1971) 91.
16 A.A. van der Giessen, Phillips Res. Repts., Suppl. 12 (1968).
17 G. Gattow and O. Glemser, Z. Anorg. Allegem. Chem., 309 (1961) 20.
18 J.A. Lee, C.E. Newnham and F.L. Tye, J. Colloid Interface Sci., 42 (1973) 370.